

# Cellular response to femtosecond-scale radiation at dose-rates exceeding $\times 10^{13}$ Gy/s.

Contact: hmaguire11@qub.ac.uk

**H. Maguire, C.A. McAnespie, E. Gerstmayr, L. Calvin, J. Sarma, G. Sarri**  
*School of Mathematics and Physics, Queen's University Belfast, BT7 1NN, Belfast, UK.*

**C. McDonnell, S.J. McMahon, K.M. Prise**  
*Patrick G. Johnston Centre for Cancer Research, Queen's University Belfast, Belfast, BT7 1NN, UK.*

**S.W. Botchway, S. Needham, O. Finlay**  
*Central Laser Facility, STFC Rutherford Appleton Laboratory, Didcot OX11 0QX, UK.*

**P. Chaudhary, G. Schettino**  
*National Physical Laboratory, Middlesex, TW11 0LW, UK.*

## Abstract

We report on the characterisation of a laser driven, very high energy electron source for radiobiological applications. This work builds on preliminary findings that demonstrated significant reduction of the relative radioresistance of cancerous tissue using this radiation source when compared to conventional radiotherapy techniques. High charge electron beams ( $\sim$ nC) were generated by a laser driven plasma wakefield accelerator allowing for dose deposition up to and exceeding 3 Gy per pulse. The electron beam duration was approximately 25 fs, equating to unprecedented mean dose-rates in excess of  $\times 10^{13}$  Gy/s. The radiation source was characterised, compared to Monte Carlo simulations and its applications to radiobiological research discussed.

## 1 Introduction

The clinical management of cancer is still a challenging problem in the twenty-first century. About 50% of cancer patients receive radiation therapy at some point during their illness, and it accounts for 40% of cancer cures [1]. The main goal of radiotherapy is to minimize the damage and exposure of normal tissue to radiation while also delivering the required dose to cancerous cells. While radiotherapy is an effective cancer treatment, it can also cause significant side effects and may fail to eliminate cancerous tissue, as cancer cells often exhibit greater radioresistance than normal tissue [2]. Continuous research into different techniques is therefore essential to achieve the best outcomes for patients.

Conventional radiotherapy techniques, which are routinely used for current radiation treatments, typically deliver low dose-rate ( $\approx 1$  Gy/min) radiation in fractions over several weeks, providing time for healthy tissue to repair between sessions. Delivery procedures are well optimized, however, this approach can still result in dam-

age to normal tissue and the therapeutic effectiveness can be limited in some cases [3]. Recently, FLASH radiotherapy (FLASH-RT) has emerged as a cutting-edge research focus in the field of radiation therapy. It has shown potential to improve outcomes by delivering high radiation doses to the treatment target in short times, equating to dose-rates much higher than that of conventional radiotherapy techniques ( $\geq 40$  Gy/s). FLASH-RT has been shown to reduce the toxicity to normal tissues while achieving comparable tumor control efficacy to conventional radiotherapy. Although the results are not yet fully understood, FLASH-RT offers a promising direction for cancer treatment [3]. Advancements in laser technologies have significantly expanded the field, enabling the development of laser-driven particle accelerators as an alternative to conventional facilities. These systems can deliver ultra-short, high dose-rate pulsed radiation sources with timescales shorter than nanoseconds [4, 5, 6]. With Gy-scale dose deposition achievable per pulse, laser-driven particle accelerators can achieve unprecedented mean dose-rates  $\geq \times 10^9$  Gy/s.

Recent advancements in laser wakefield acceleration (LWFA) have enabled the routine generation of very high energy electron (VHEE) beams ( $\geq 100$  MeV) with high charge ( $\geq 1$  nC) and pulse durations as short as tens of femtoseconds [7]. Since the late 1990s, VHEEs have been proposed for the treatment of deep-seated tumors [8]. VHEEs can achieve excellent dose conformity due to their dose distributions and deep penetration depths, which is attributed to their high inertia. This makes them comparable to, if not better than, current treatment modalities [9, 10]. Theoretical studies indicate that VHEEs can enhance the sparing of critical structures while providing similar or superior target coverage than photons, with reduced susceptibility to tissue inhomogeneities [11, 12, 13]. More recent Monte Carlo and experimental studies showed that by externally focusing the electron beam using a magnetic lens, the depth-dose

profile of a collimated VHEE beam, which is almost uniform, results in a profile that resembles a degraded Bragg peak. These focused VHEE beams concentrate dose into a well-defined volume deep in tissue reducing surface and exit doses [14, 15, 16]. These findings point to a new, promising direction in radiobiological research.

Knowledge and understanding of DNA damage and repair following irradiation with laser-driven electron beams remains limited due to variations between the radiation source. Some literature report on the accumulation of multiple pulses delivering mGy to cGy doses utilising low energy electrons [17, 18, 19] and VHEEs [20], while others report on single pulses of low energy electrons with sub-picosecond durations [21] and nanosecond durations [22]. Recent work by our group and the work presented in this report extends on the above literature, utilising femtosecond pulses of VHEEs with each pulse delivering Gy-scale doses, marking a significant advancement in the field. Preliminary results, when delivering laser driven, ultra short, VHEE beams onto cell samples, show significant reduction of the relative radioresistance of cancerous tissue compared to conventional radiotherapy methods [4]. The extremely short duration of these beams approaches timescales comparable to the initial cellular response to ionising radiation, allowing possible novel phenomena in radiobiology to be investigated [23].

Building on the preliminary studies which demonstrated the potential of a LWFA VHEE source as a platform for femtosecond-scale, radiobiological research, this study expanded on initial results by irradiating seven different cell lines (five cancerous and two healthy). The goal was to confirm that the enhanced killing of cancerous cells with ultra-short electron beams, compared to conventional radiotherapy techniques, is consistent across all cell lines and independent of cell type.

## 2 Experiment set-up

Figure 1 shows a schematic of the experimental set-up used at the Gemini laser, Central Laser Facility, UK, which delivered laser pulses with  $(6.3 \pm 0.3)$  J of energy in  $(45 \pm 5)$  fs. The normalised laser intensity was measured as  $a_0=1.4\pm0.1$ . The laser was focused using a F/40 off-axis parabola 5 mm above a 15 mm long supersonic gas-jet where a 2% nitrogen in helium gas target was used.

The energy spectrum of the accelerated electrons was obtained using a magnetic spectrometer consisting of a removable 30 cm, 1T dipole magnet and two LANEX scintillator screens. Two LANEX screens, L1 and L2, were used to capture the full range of energies, detecting higher and lower energy electrons, respectively. A Mu-metal tube was installed on the dipole magnet to shield on-axis electron shots from fringe fields.

A Kapton and Kevlar window (with  $130\mu\text{m}$  and  $370\mu\text{m}$  thicknesses, respectively) was used to allow the

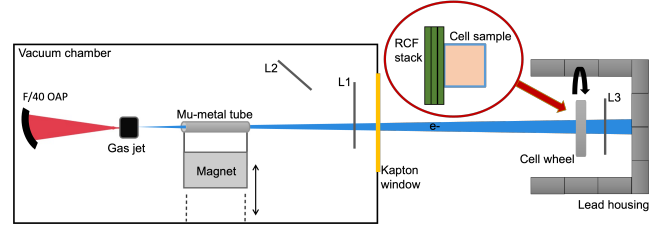


Figure 1: Simplified schematic of the experimental set-up. The magnetic spectrometer consists of a removable 1T dipole magnet and two Lanex screens, L1 and L2. A third LANEX screen, L3 is positioned behind the cell wheel to obtain online dose profiles of the electron beam for on axis-shots.

propagation of the electrons from the vacuum chamber into the cell irradiation area. A removable set of 1mm PTFE and 1mm Fe plates were placed directly after the Kapton window to increase the divergence of beam- required for some cell analysis. The residual laser beam was dumped onto a 1 mm ceramic screen positioned inside the vacuum chamber. Up to 10 cell samples were placed in the sample wheel, which was rotated to irradiate different samples after each shot. A third dose-calibrated LANEX screen, L3, was positioned behind the cell wheel to provide online dose profile measurements during optimization and characterization. Each cell sample had a stack of three RCFs facing the electron beam to obtain final absolute dose measurements from the optimised electron beam.

## 3 Main results

Figure 2 shows the electron energy spectra for 10 shots with the mean displayed as the thick black line and standard deviation represented by the grey shading. The mean charge of the electron beam,  $N_e$ , was  $1.8 \pm 0.3$  nC.

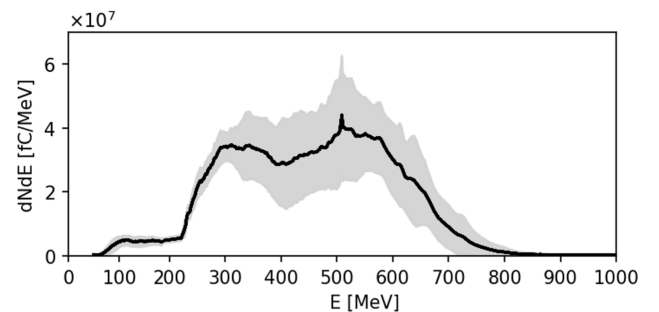


Figure 2: The angularly integrated spectra of 10 consecutive shots at different energies in MeV. The mean of these 10 shots is displayed as the black line, with the standard deviation as the grey shading.

The maximum duration of LWFA electron beams can be estimated to be on the order of the plasma bub-

ble radius, which can be estimated as  $r_b/c = 2\sqrt{a_0}/\omega_p$  where  $c$  and  $\omega_p$  are the speed of light and plasma frequency, respectively [24]. Using the electron plasma density  $n_e$ , which was measured via optical interferometry as  $(2.8 \pm 0.2) \times 10^{18} \text{ cm}^{-3}$ , the plasma frequency  $\omega_p$  was calculated. Along with the  $a_0$  stated above, the electron bunch duration  $\tau_e$  was estimated to be  $25 \pm 1.8 \text{ fs}$ .

The dosimetric properties of these beams were measured when the magnet was retracted off-axis. The dose measured on the LANEX screen for 12 consecutive shots is shown in figure 3. It is clear that the electron beam exhibits both shot-to-shot pointing and dose fluctuations. This pointing fluctuation can be attributed to the pointing of the LWFA laser, shot-to-shot instabilities in the plasma channel and fluctuations in laser parameters [25]. The root-mean-square deviation in electron beam pointing was measured to be  $2.40 \text{ mrad}$  and the divergence of the electron beam was measured to be  $1.44 \pm 0.42 \text{ mrad}$ .

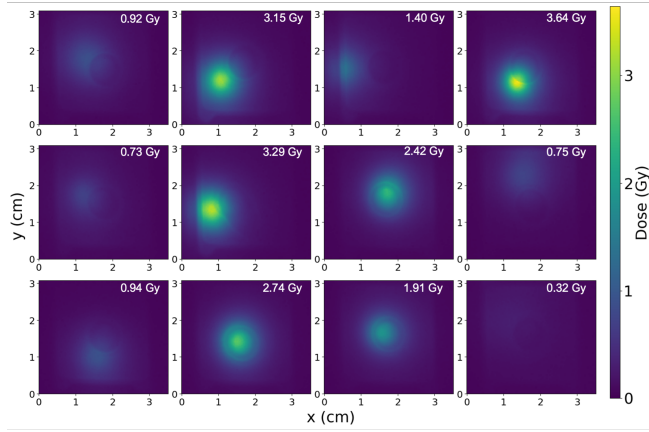


Figure 3: Dose profiles and pointing stability obtained from the LANEX screen behind the cell samples for 12 consecutive shots after optimisation. The peak dose for each shot is printed in white.

For certain cellular analysis techniques, a larger irradiation area was required. This was achieved by the addition of 1mm PTFE and 1mm Fe plates at the exit of the vacuum chamber. Monte Carlo simulations using the TOPAS (Geant4) code were run to fully characterise the effect that the addition of the two plates had to the electron beam. In the simulations, the electron beam was input with a custom energy spectrum using the average of the measured electron spectra in figure 2. The beam divergence was input as stated above and the cell sample was replaced with a  $1.5 \times 1.5 \times 10 \text{ cm}$  water phantom, split into  $50 \mu\text{m}^3$  voxels for dose scoring in the transverse and longitudinal directions. The simulations were run with  $10^7$  primaries, and the results scaled to match the measured electron beam charge.

Figure 4 shows RCF measurements for when the two plates were removed and inserted, alongside the corre-

sponding TOPAS simulation results.

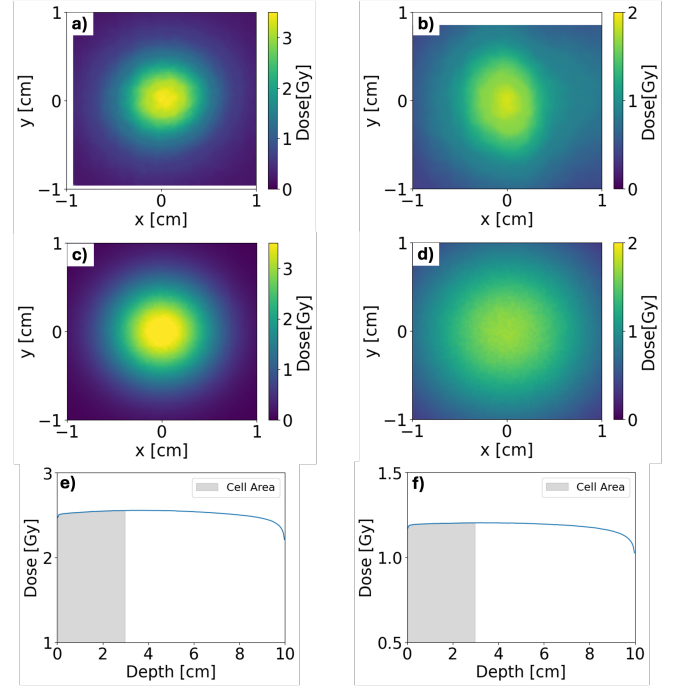


Figure 4: Dose profiles from RCF measurements (a, b) and corresponding TOPAS simulations (c, d). Depth-dose curves are shown in (e, f), with the cellular irradiation area highlighted in grey. Results without the PTFE and Fe plates are displayed on the left (a, c, e), while results with the plates are shown on the right (b, d, f).

The full-width half-maximum (FWHM) of the electron beam, visible in figure 4 (a), was measured to be  $0.92 \text{ cm} \times 0.94 \text{ cm}$ . This measured value from the RCF is well in agreement with the simulated values of  $0.92 \text{ cm} \times 0.93 \text{ cm}$  as seen in figure 4 (c). The average doses across the FWHM region were  $2.2 \text{ Gy}$  and  $2.6 \text{ Gy}$  for measured and simulated results, respectively. Figure 4 (e) shows this average dose value along the cell sample in the longitudinal direction, where the variation of dose in the shaded cell area region was  $0.61\%$ . The results following the insertion of the PTFE and Fe plates can be seen in figures 4 (b, d, f). The measured FWHM values show an increase of  $54\%$  to  $1.42 \text{ cm} \times 1.43 \text{ cm}$  as well as a  $43\%$  increase in the simulated results to  $1.31 \text{ cm} \times 1.32 \text{ cm}$ . The average dose values were effectively halved with measured and simulated results of  $1.1 \text{ Gy}$  and  $1.3 \text{ Gy}$ , respectively. The variation in average dose in the longitudinal direction in the cell area was  $0.43\%$ .

It was important to verify that the insertion of the two plates into the setup did not generate significant amounts of bremsstrahlung radiation. TOPAS simulations showed that the addition of the two plates to the set-up resulted in a  $0.31\%$  rise in gamma radiation contribution to the total dose deposited in the cell region, compared to the setup without the plates. Overall, the

dose deposited by gamma radiation on the cell plane was in the range of 20-30mGy, which was a negligible fraction ( $\sim 1\%$ ) of the maximum dose delivered by the electron beams.

Shot-to-shot stability of all the beam parameters is of crucial concern for real clinical applications. We observed the beam charge to be rather stable when averaged over 10 laser shots, however, the dose and beam pointing are quite variable. This in turn limits the application of this source to radiobiological studies, which require strict spatial and dosimetric properties for effective measurements of biological outcomes. That being said, we successfully mapped the dose to the irradiated cell area and conducted clonogenic cell assays as well as 53BP1 foci induction assays (to measure DNA double-strand break repair, as seen in figure 5) similar to before [4], to quantify the effect that this radiation source has on biological samples.

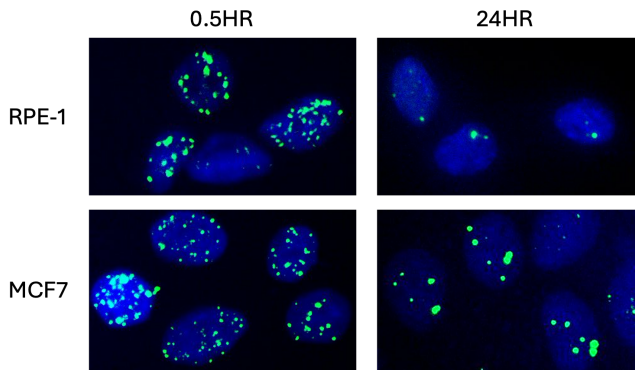


Figure 5: **53BP1 Foci Formation.** Foci distributions as functions of time (0.5hr, 24hr after irradiation) for RPE-1, a healthy cell line, and MCF7, a cancerous cell line. Shown are merged channel images of 53BP1 DNA DSB marker (green) and DAPI nuclear stain (blue).

## 4 Conclusions

Our study presents a comprehensive characterisation of a laser driven electron beam produced by the Gemini laser. Our results show that doses exceeding 3 Gy can be attained within an estimated 25 fs pulse duration. With Gy-scale dose deposition in a femtosecond pulse, this electron source enables unprecedented dose-rates in excess of  $\times 10^{13}$  Gy/s to be achieved. The duration of the electron beam aligns with the initial cellular response to ionising radiation, allowing for a unique regime of radiobiological research to be investigated.

## References

[1] Rajamanickam Baskar et al. Cancer and Radiation Therapy: Current Advances and Future Directions. *Int J Med Sci* **9**, (2012), pp. 193–199.

[2] D. I. Thwaites J. R. Williams. Radiotherapy Physics in Practice. *Oxford University Press*, 407-450 (2000).

[3] Rui Tang et al. FLASH radiotherapy: A new milestone in the field of cancer radiotherapy. *Cancer Letters* **587**, (2024), p. 216651.

[4] C. A. McAnespie et al. Single-pulse Gy-scale irradiation of biological cells at average dose-rates above  $10^{13}$  Gy/s from a laser-wakefield accelerator (2024). arXiv: 2409.01717 [physics.med-ph].

[5] Pankaj Chaudhary et al. Radiobiology experiments with ultra-high dose rate laser-driven protons: methodology and state-of-the-art. *Frontiers in Physics* **9**, (2021), p. 624963.

[6] Sean McCallum et al. Proof-of-Principle of Absolute Dosimetry Using an Absorbed Dose Portable Calorimeter with Laser-Driven Proton Beams. *Applied Sciences* **13**, 21 (2023), p. 11894.

[7] Hyung Taek Kim et al. Multi-GeV Laser Wakefield Electron Acceleration with PW Lasers. *Applied Sciences* **11**, 13 (2021).

[8] Lech Papiez, Colleen DesRosiers, and Vadim Moskvina. Very high energy electrons (50–250 MeV) and radiation therapy. *Technology in cancer research & treatment* **1**, 2 (2002), pp. 105–110.

[9] Anna Subiel et al. Challenges of dosimetry of ultra-short pulsed very high energy electron beams. *Physica Medica* **42**, (2017), pp. 327–331.

[10] Alexander Hart et al. Plastic scintillator dosimetry of ultra-high dose-rate 200 MeV electrons at CLEAR. *IEEE Sensors Journal* (2024), pp. 1–1.

[11] Vadim Moskvina et al. “PENELOPE Monte Carlo engine for treatment planning in radiation therapy with Very High Energy Electrons (VHEE) of 150–250 MeV”. *IEEE Nuclear Science Symposium Medical Imaging Conference*. 2010, pp. 1961–1966.

[12] B Palma et al. MO-FG-303-06: Evaluation of the performance of very high-energy electron (VHEE) beams in radiotherapy: Five clinical cases. *Medical physics* **42**, 6Part29 (2015), pp. 3568–3568.

[13] Agnese Lagzda et al. “Relative insensitivity to inhomogeneities on very high energy electron dose distributions”. *Proc. 8th Int. Particle Accelerator Conf. (IPAC’17)*. 2017.

[14] K. Kokurewicz et al. Focused very high-energy electron beams as a novel radiotherapy modality for producing high-dose volumetric elements. *Sci. Rep.* **9**, 1 (2019), p. 10837.

[15] Karolina Kokurewicz et al. An experimental study of focused very high energy electron beams for radiotherapy. *Communications Physics* **4**, 1 (2021), p. 33.

[16] Lucy Whitmore et al. Focused VHEE (very high energy electron) beams and dose delivery for radiotherapy applications. *Scientific Reports* **11**, 1 (2021), p. 14013.

[17] Maria Grazia Andreassi et al. Radiobiological effectiveness of ultrashort laser-driven electron bunches: Micronucleus frequency, telomere shortening and cell viability. *Radiation research* **186**, 3 (2016), pp. 245–253.

[18] Elke Beyreuther et al. Radiobiological response to ultra-short pulsed megavoltage electron beams of ultra-high pulse dose rate. *International Journal of Radiation Biology* **91**, 8 (2015), pp. 643–652.

[19] Melanie Oppelt et al. Comparison study of in vivo dose response to laser-driven versus conventional electron beam. *Radiation and environmental biophysics* **54**, (2015), pp. 155–166.

- [20] Stefana Orobeti et al. First in vitro cell co-culture experiments using laser-induced high-energy electron FLASH irradiation for the development of anti-cancer therapeutic strategies. *Scientific Reports* **14**, (2024).
- [21] O Rigaud et al. Exploring ultrashort high-energy electron-induced damage in human carcinoma cells. *Cell death & disease* **1**, 9 (2010), e73–e73.
- [22] Santhosh Acharya et al. Dose rate effect on micronuclei induction in human blood lymphocytes exposed to single pulse and multiple pulses of electrons. *Radiation and environmental biophysics* **50**, (2011), pp. 253–263.
- [23] Luca Labate et al. Toward an effective use of laser-driven very high energy electrons for radiotherapy: Feasibility assessment of multi-field and intensity modulation irradiation schemes. *Scientific Reports* **10**, (Oct. 2020), p. 17307.
- [24] Alexander George Roy Thomas. Scalings for radiation from plasma bubbles. *Physics of Plasmas* **17**, 5 (2010).
- [25] Stefan Karsch et al. GeV-scale electron acceleration in a gas-filled capillary discharge waveguide. *New Journal of Physics* **9**, 11 (2007), p. 415.